Simultaneous observations of ions of ionospheric origin over the ionosphere and in the plasma sheet at storm-time substorms

M. Nosé, T. Kunori, Y. Ono, S. Taguchi, K. Hosokawa, T. E. Moore, M. R. Collier, S. P. Christon, and R. W. McEntire

Abstract: We investigate variations of ion flux over the ionosphere and in the plasma sheet when storm-time substorms are initiated, using simultaneous observations of neutral atoms in the energy range of up to a few keV measured by the low-energy neutral atom (LENA) imager on board the Imager for Magnetopause-to-Aurora Global Exploration (IMAGE) satellite and energetic (9-210 keV/*e*) ion flux measured by the energetic particle and ion composition (EPIC) instrument on board the Geotail satellite. We examined three storm intervals during which the IMAGE satellite was located near its apogee and the Geotail satellite was in the plasma sheet on the nightside. Low-energy neutral atoms traveling from the direction of the Earth can be created by outflowing ionospheric ions through charge exchange processes. The observed neutral atom flux enhancement at storm-time substorms indicates that substorms can cause an immediate increase of low-energy ion flux over the ionosphere by a factor of 3-10. In the plasma sheet, the flux ratio of O^+/H^+ is rapidly enhanced at storm-time substorms and then increased gradually or stayed at a constant level in a timescale of $\sim$60 minutes, suggesting a mass-dependent acceleration of ions at local dipolarization and a subsequent additional supply of O^+ ions to the plasma sheet which have been extracted from the ionosphere at the substorms.

Key words: Ions of Ionospheric Origin, Substorms, Plasma Sheet, Ion Acceleration.

1. Introduction

Recent studies revealed the ionosphere as an important source of plasma to the plasma sheet and the magnetosphere. From multi-fluid MHD simulation *Winglee* [1998] has shown that a boundary called "the density geopause," within which the ionospheric source is the dominant contributor to the plasma, is extended down the tail to 10-65 R_E during the southward IMF (B_Z=0 to -5 nT). A large number of numerical simulations were performed to trace ions of ionospheric origin after they escaped from the ionosphere [e.g., *Delcourt et al.*, 1999; *Chappell et al.*, 2000; *Cully et al.*, 2003a]. They found that most of such ions preferentially move into the plasma sheet through the geomagnetic lobe. Thus it is important to identify how much ions of ionospheric ions are outflowing from the ionosphere and how it depends on the geomagnetic disturbances. Using the Dynamic Explorer -1 observation of low-energy (0.01-17 keV) ions, *Yau et al.* [1988] found a good correlation between the ion outflow rate and the Kp index. As the Kp index increased from 0 to 6, the O^+ flux increased drastically by an order (from 1-3$\times10^{25}$ s^{-1} to 1-3$\times10^{26}$ s^{-1}), while the H^+ flux changed by a factor of $\sim$3 (from 3$\times10^{25}$ s^{-1} to 1$\times10^{26}$ s^{-1}). From observations by the EXOS-D satellite of ion outflow in the energy range from $<$1 to 70 eV, *Cully et al.* [2003b] showed that ion outflow rate is correlated with the Kp index and some solar wind parameters. The Kp dependence of H^+ and O^+ flux was almost similar to that by *Yau et al.* [1988]. They also found that the solar wind parameters exhibiting a strong correlation with the outflow flux were the kinetic pressure, the electric field, and the variation in the IMF. In these studies the 3-hour Kp index or the hourly averaged solar wind data (OMNI data) have been used, suggesting that the reported good correlation is correct only in a statistical or average sense. It is not clear yet how outflowing ion flux responds to geomagnetic disturbances with a shorter timescale ($<$1 hour) such as substorms.

In this study we intended to investigate how ion outflow rate changes at individual substorms, using data obtained by the low-energy neutral atom (LENA) imager on board the Imager for Magnetopause-to-Aurora Global Exploration (IMAGE) satellite. Since IMAGE/LENA is a remote sensing instrument, it provides a global image of outflowing ion flux over the polar region with a time resolution of $\sim$2 minutes. We can monitor temporal changes of outflowing ion flux when a substorm occurs. Moreover, in order to investigate how the plasma sheet ion composition responds to the identical substorm, we examined simultaneous observations of energetic (9-210 keV/*e*) ion flux in the plasma sheet made by the energetic particle and ion composition (EPIC) instrument on board the Geotail satellite. The rest of this paper is organized as follows. Section 2 introduces the data set. In section 3 we describe the event selection procedure. We found 3 time intervals during which the IMAGE and Geotail satellites simultaneously ob-

Received 15 May 2006.

M. Nosé,[1] T. Kunori, and Y. Ono. Graduate School of Science, Kyoto University, Kyoto, Japan
S. Taguchi and K. Hosokawa. Department of Information and Communication Engineering, University of Electro-Communications, Tokyo, Japan
T. E. Moore and M. R. Collier. NASA Goddard Space Flight Center, Greenbelt, Maryland, USA
S. P. Christon. Focused Analysis and Research, Columbia, Maryland, USA
R. W. McEntire. Applied Physics Laboratory, Johns Hopkins University, Laurel, Maryland, USA

[1]Corresponding author (e-mail: nose@kugi.kyoto-u.ac.jp).

served ions of ionospheric origin. In section 4 satellite observations will be displayed for the intervals 1 and 3. It was found that substorms caused rapid increases of both the energetic neutral atom (ENA) flux around the Earth and the O^+/H^+ energy density ratio in the plasma sheet. The O^+/H^+ ratio subsequently increased or stayed at a constant level with a timescale of 60 minutes. We will discuss these observational results in section 5.

2. Data Set

The IMAGE satellite is a polar orbiting satellite with a perigee of 1000 km altitude, an apogee of 8.2 R_E, and an orbital period of 14.2 hours [*Burch*, 2000]. The satellite spins at a rate of $\sim$0.5 revolution per minute and its spin vector is anti-parallel to the orbital angular momentum vector. The LENA imager carried by the IMAGE satellite is designed to detect neutral atoms in the energy range of $\sim$10 eV to a few keV and has a field of view of $\pm 45^\circ$ against a satellite spin plane which is divided by 12 polar sectors [*Moore et al.*, 2000]. Because of the spin, the LENA imager sweeps out 360° in azimuthal direction, which is divided by 45 azimuthal sectors, resulting in one complete image of neutral atom flux covering an area of 90°(polar)$\times 360^\circ$(azimuth) at every 2 minutes. Since low-energy neutral atoms traveling from the direction of the Earth are created by outflowing ionospheric ions through charge exchange processes, we can investigate temporal change of the low-energy ion flux over the ionosphere from the LENA data.

The Geotail satellite was placed in the near-Earth orbit of $\sim 9 \times 30$ R_E in the fall of 1994 [*Nishida*, 1994] and surveys the near-Earth and midtail plasma sheet frequently. Geotail is equipped with the EPIC instrument which provides mass and charge state information about ions with an energy/charge range of 9 keV/*e* to 210 keV/*e* in eight spectral points [*Williams et al.*, 1994]. The instrument has a spatial coverage of almost 4π sr. It takes $\sim$24 s to get one complete energy spectrum for H^+ ions, and $\sim$48 s for O^+ ions. From each energy spectrum we calculated energy densities of H^+ and O^+, and then averaged over 5 min to increase statistical significance. We also used the magnetic field data obtained by the magnetic field (MGF) instrument [*Kokubun et al.*, 1994] onboard the Geotail satellite.

3. Event Selection

From the period of August 2003 through July 2004, we selected time intervals during which IMAGE/LENA and Geotail/EPIC made a simultaneous observation of ions of ionospheric origin, according to the following criteria. During the time interval, (1) geomagnetic storms took place, (2) the Geotail satellite mostly stayed in the nightside plasma sheet, (3) the IMAGE satellite was near its apogee, and (4) clear substorm signatures can be identified by ground stations and geosynchronous satellites. This selection procedure yielded 3 time intervals, that is, 1900-2300 UT on 30 October 2003 (interval 1), 0130-0600 UT on 27 July 2004 (interval 2), and 0400-0730 UT on 10 March 2004 (interval 3). Figure 1 shows orbits of the satellites in the X_{GSM}-Y_{GSM} and X_{GSM}-Z_{GSM} planes for these 3 intervals. Thin lines indicate the IMAGE orbits and thick lines indicate the Geotail orbits. Geotail flew at $X_{GSM} \sim$-8, -16, and -24 R_E in the interval 1, 2, and 3, respectively. In the next section we will show simultaneous observations for the interval 1 and 3; data of the interval 2 will be omitted because of limit of paper length.

4. Observation and Analysis

4.1. Interval 1 (1900-2300 UT on 30 October 2003)

During this interval the SYM-H index decreased from -150 nT to -400 nT, indicating the main phase of the very intense magnetic storm. Substorms were identified at 1947 UT and 2115 UT by energetic electron enhancement at geosynchronous satellites, negative bays at high-latitude ground stations, and positive bays at mid-latitude ground stations (not shown here). Figures 2a and 2b show the ENA images around the Earth obtained by the IMAGE/LENA imager before and after the first substorm onset (1947 UT), respectively. We found that ENA flux coming from the direction of the Earth was enhanced. ENA images before and after the second substorm onset (2115 UT) are shown in Figures 2c and 2d. We also found strong ENA flux enhancement after the substorm onset. In order to

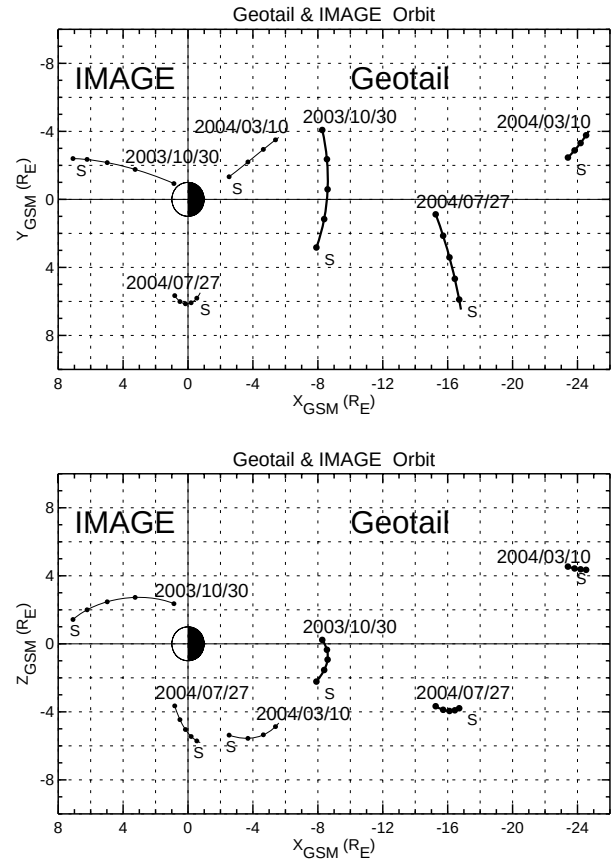

Fig. 1. Orbits of the IMAGE and Geotail satellites in the X_{GSM}-Y_{GSM} (top) and X_{GSM}-Z_{GSM} (bottom) planes for the 3 selected intervals. Thin and thick lines are for the IMAGE and Geotail orbits, respectively. Dots indicate the satellite locations at integer hour. "S" denotes the start location of the satellite in the interval.

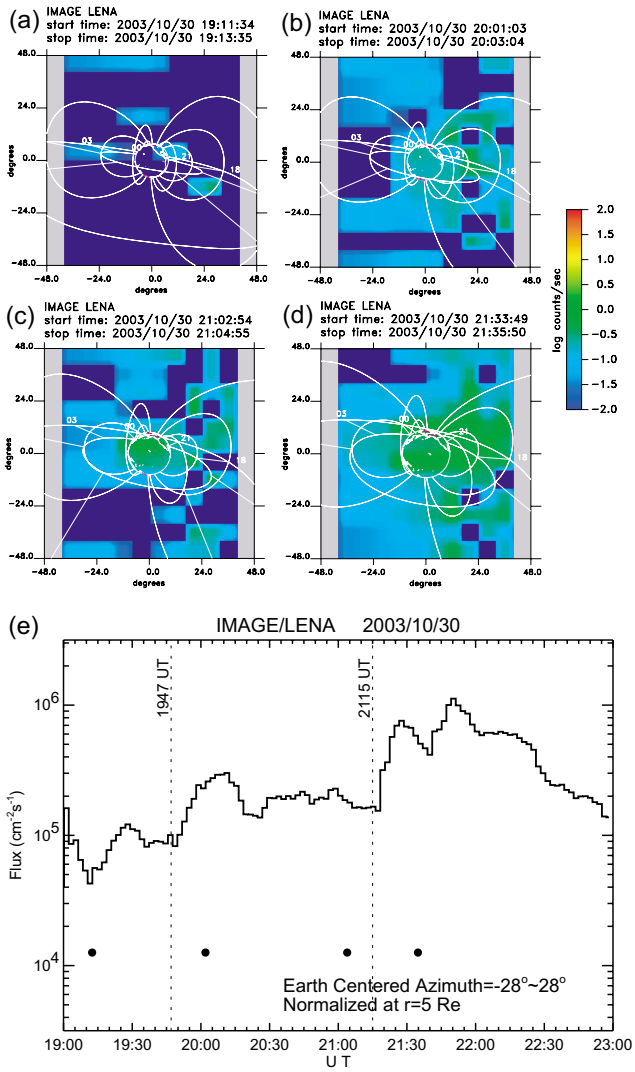

Fig. 2. (a, b) ENA images around the Earth obtained by the IMAGE/LENA imager before and after the first substorm onset. (c, d) The same as Figure 2a and 2b, except for the second substorm onset. (e) Temporal variations of the ENA flux around the Earth. Onset times of the substorms were indicated by vertical dashed lines. Four black circles indicate times of Figures 2a-2d.

see temporal changes of the ENA flux in more detail, we averaged the ENA flux around the Earth over the azimuthal angle of $\pm 28^\circ$ (y-direction of the ENA image) and the polar angle of $\pm 44^\circ$ (x-direction of the image). Then we computed the normalized ENA flux ($J_{\rm normalized}$) from the average ENA flux derived above ($J_{\rm averaged}$) as it is measured at radial distance of 5 R_E, by

$$J_{\rm normalized} = J_{\rm averaged} \times \left(\frac{r - 1.5}{5 - 1.5} \right)^2 ,$$

where r is the radial distance of the satellite position in R_E. Here the ENA source was assumed to be at geocentric altitude of 1.5 R_E [*Khan et al.*, 2003]. This generates time series data of ENA flux around the Earth with a time resolution of 2 minutes. We calculated a running average of $J_{\rm normalized}$ with a time window of 8 minutes, which is displayed in Figure 2e. Vertical dashed lines indicate onset time of the substorms. Black circles corresponds to times in which the LENA images of Figures 2a-2d were taken. At the first substorm the ENA flux was clearly enhanced from 1×10^5 cm^{-2}s^{-1} to 3×10^5 cm^{-2}s^{-1} within 20 minutes. The second substorm was accompanied by a sudden increase of the ENA flux from 2×10^5 cm^{-2}s^{-1} to 1×10^6 cm^{-2}s^{-1}. This indicates that the substorms caused an enhancement of outflowing ion flux by a factor of 3-5.

Figure 3 showed the magnetic field in the X_{GSM} and Z_{GSM} components and the O^+/H^+ energy density ratio measured by the Geotail satellite which was located at $X_{GSM}\sim$-8 R_E (Figure 1). Two vertical lines indicate onset time of the substorms (1947 UT and 2115 UT). At the fist substorm onset, the absolute value of B_X decreased and B_Z increased, indicating that dipolarization took place. At the same time the O^+/H^+ energy density ratio increased suddenly from $\sim$1 to 3, and then it showed a gradual increase during 2000-2030 UT, even though the substorm expansion phase has already ended at 2000-2010 UT as can be seen in B_Z changes. For the second substorm onset, signatures of the magnetic field and the O^+/H^+ energy density ratio were similar to those of the first substorm; that is, the magnetic field was dipolarized and the energy density ratio increased rapidly at substorm onset, followed by a gradual increase with a timescale of 60 minutes (2130-2230 UT).

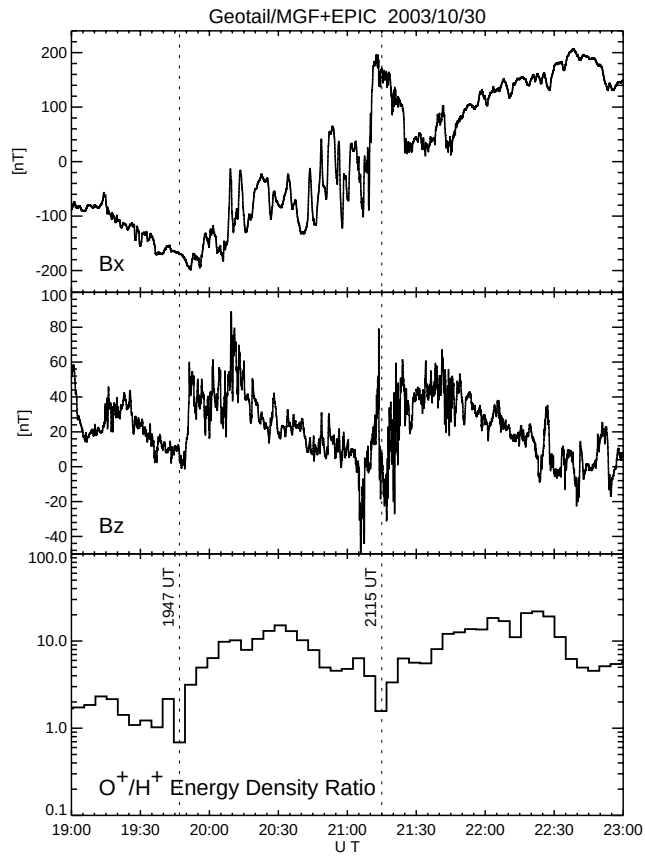

Fig. 3. From top to bottom: The magnetic field in the X_{GSM} and Z_{GSM} components, and the O^+/H^+ energy density ratio measured by the Geotail satellite.

4.2. Interval 3 (0400-0730 UT on 10 March 2004)

This interval was found in the recovery phase of a moderate magnetic storm and the SYM-H index was between -100 nT and -60 nT. We identified occurrence of a substorm at 0528 UT by dipolarization and energetic proton enhancement at geosynchronous satellites, a negative bay at high-latitude ground station, and a positive bay at low-latitude ground station (not shown here). Figures 4a and 4b display the IMAGE/LENA image around the Earth before and after the substorm. It was revealed that the ENA flux traveling from the direction of the Earth was enhanced after the substorm. Figure 4c shows ENA flux variations derived in the same way as Figure 2e. A vertical line and two black circles indicate times when substorm occurred and the LENA images of Figures 4a and 4b were taken. The ENA flux before the substorm stayed around 1×10^4 cm^{-2}s^{-1}, while it increased up to 1×10^5 cm^{-2}s^{-1} within 10-20 minutes after the substorm, indicating an enhancement of outflowing ion flux by a factor of 10.

Figure 5 demonstrates the Geotail data at $X\sim$-24 R_E in the same format as Figure 3. At the substorm, which is indicated by a vertical line, the absolute value of B_X decreased and B_Z increased, being a dipolarization signature. For about 1 hour prior to the substorm onset (i.e., 0430-0528 UT), Geotail was in the magnetic lobe and we could not calculate the energy density ratio in the plasma sheet. However, before 0430 UT the satellite made a measurement of energetic ion flux in the plasma sheet, which indicates the O^+/H^+ ratio of 0.02-0.05. Assuming that the O^+/H^+ energy density ratio did not change significantly before the substorm onset, we can expect that the

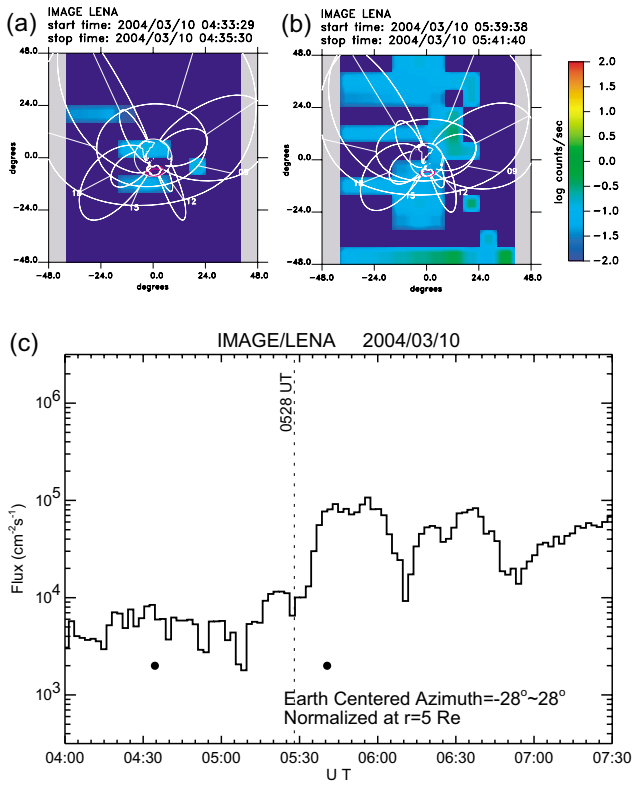

Fig. 4. The same as Figure 2, except for the interval 3.

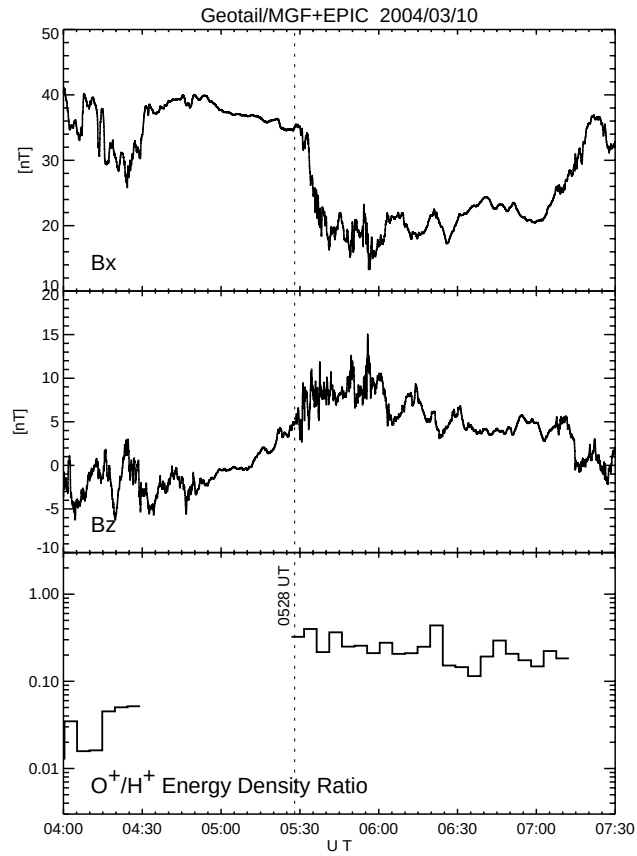

Fig. 5. The same as Figure 3, except for the interval 3.

energy density ratio was strongly enhanced at dipolarization. Even though the substorm expansion phase has ended around 0550-0600 UT as can be noted from the magnetic field data, the O^+/H^+ energy density ratio stayed at almost constant level of 0.2-0.3 for about 1 hour.

5. Discussion

We examined variations of ions of ionospheric origin over the ionosphere and in the plasma sheet when storm-time substorms were initiated. From the IMAGE/LENA observation we found that the ENA flux around the Earth was enhanced rapidly (within 10-20 minutes) by a factor of 3-10 at substorms. (Substorms in the interval 2 were also accompanied by the ENA flux enhancement in the similar way to those in the interval 1 and 3.) The Geotail/EPIC observation showed that the O^+/H^+ energy density ratio in the plasma sheet was immediately enhanced when local dipolarization signatures appeared, and then increased gradually or stayed at nearly constant level in a timescale of 60 minutes. These Geotail observations were similar among three different locations of $X_{GSM}\sim$-8, -16, and -24 R_E, though data at $X_{GSM}\sim$-16 R_E were not shown here because of page limit.

5.1. Response of outflowing ion flux to substorms

From the IMAGE/LENA observations we suppose that substorms can cause sudden and drastic changes of the ion flux

outflowing from the Earth. Since this flux change caused by substorms is nearly comparable to that during Kp increase from 0 to 6 (i.e., threefold to tenfold) which was statistically revealed by *Yau et al.* [1988] and *Cully et al.* [2003b] (see section 1), it is important to take substorm occurrence into consideration when we study outflowing ion flux. We can expect that such drastic change of outflowing ion flux at substorms possibly affect ion composition in the plasma sheet; this issue will be discussed in section 5.2.

It is noteworthy to mention prompt response of outflowing ion flux to the solar wind dynamic pressure, which has been described by *Moore et al.* [1999], *Fuselier et al.* [2002], and *Khan et al.* [2003]. They reported that enhancements of solar wind dynamic pressure (or standard deviation of dynamic pressure) led to bursts of ion outflow. Their results might be explained by that enhancement of the solar wind dynamic pressure preferentially triggers substorms [*Kokubun et al.*, 1977]. In actual fact, the two substorms in the interval 1 appeared to be associated with strong compression of the magnetosphere during high solar wind dynamic pressure, as discussed by *Nosé et al.* [2005].

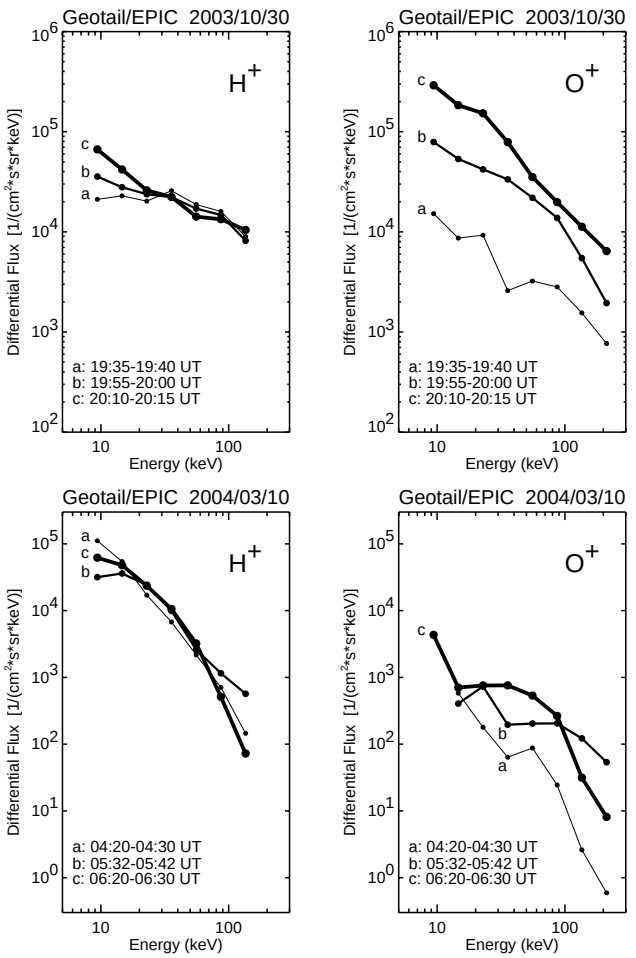

Fig. 6. Energy spectra of H^+ and O^+ observed by Geotail/EPIC during the first substorm in the interval 1 (top) and the substorm in the interval 3 (bottom). Light line is for the spectra before the onset; medium line, 10-15 minutes after the onset; and heavy line, 30-60 minutes after the onset.

At the substorm onset in the interval 3 there was a weak dynamic pressure enhancement (from 6 nPa to 7 nPa) which is due to slight solar wind velocity enhancement (from 650 km/s to 700 km/s). On the other hand, we found that there were no clear pressure changes at substorms in the interval 2, but rather there were northward turnings of the IMF with an amplitude of 10-20 nT. It is left for future study to examine which solar wind dynamic pressure enhancement or substorm is more essential to the immediate increases of the ionospheric plasma outflow.

5.2. Ion composition change in plasma sheet

We consider that the first sudden enhancement of the O^+/H^+ energy density ratio in the plasma sheet is caused by mass-dependent acceleration of ions at dipolarization and the subsequent gradual increase of the energy density ratio is due to an additional supply of O^+ ions which are extracted from the ionosphere at the substorm onset. This idea is supported by energy spectral changes observed by the Geotail/EPIC instrument. Top two panels of Figure 6 display H^+ and O^+ energy spectra in the plasma sheet for the substorm onset at 1947 UT on 30 October 2003 (the first onset in the interval 1), and bottom two panels, for the substorm onset at 0528 UT on 10 March 2004 (the onset in the interval 3). Different line width means different time intervals; that is, light, medium, and heavy lines represent energy spectra before onset, 10-15 minutes after onset, and 30-60 minutes after onset, respectively. It was found that the H^+ energy spectra did not show significant changes in both substorm onsets. However, the O^+ energy spectra changed drastically at the energy range of a few tens of keV to 100 keV after dipolarization (medium line), implying that acceleration of ions was more effective to O^+ ions than H^+ ions. At 30-60 minutes after the onset, we found that O^+ flux in lower energy range from 9 keV to a few tens of keV showed a further increase (heavy line). The O^+ increase in the lower energy range can be explained by that extra O^+ ions are transported into the plasma sheet within 60 minutes after they are extracted from the ionosphere at substorm onset as confirmed from the LENA observations (Figures 2 and 4). This timescale is consistent with previous studies showing that transit time of ions from the ionosphere to the plasma sheet via the magnetic lobe is $\leq$1-2 hours [*Cladis*, 1986; *Delcourt et al.*, 1999; *Chappell et al.*, 2000].

Acknowledgements

We thank D. J. Williams and S. R. Nylund for their help in processing the Geotail/EPIC data. We also thank T. Nagai for providing the Geotail/MGF data. This work was supported by the Sumitomo Foundation (grant 030677) and the Ministry of Education, Science, Sports and Culture, Grant-in-Aid for Young Scientists (B) (grant 17740327).

References

1. Burch, J. L., IMAGE mission overview, *Space Sci. Rev.*, 91, 1-14, 2000.
2. Chappell, C. R., B. L. Giles, T. E. Moore, D. C. Delcourt, P. D. Craven, and M. O. Chandler, The adequacy of the ionospheric

source in supplying magnetospheric plasma, *J. Atmos. Sol. Terr. Phys.*, *62*, 421-436, 2000.
3. Cladis, J. B., Parallel acceleration and transport of ions from polar ionosphere to plasma sheet, *Geophys. Res. Lett.*, *13*, 893-896, 1986.
4. Cully, C. M., E. F. Donovan, A. W. Yau, and H. J. Opgenoorth, Supply of thermal ionospheric ions to the central plasma sheet, *J. Geophys. Res.*, *108*, 1092, doi:10.1029/2001JA009457, 2003a.
5. Cully, C. M., E. F. Donovan, A. W. Yau, and G. G. Arkos, Akebono/Suprathermal Mass Spectrometer observations of low-energy ion outflow: Dependence on magnetic activity and solar wind conditions, *J. Geophys. Res.*, *108*, 1093, doi:10.1029/2001JA009200, 2003b.
6. Delcourt, D. C., N. Dubouloz, J.-A. Sauvard, and M. Malingre, On the origin of sporadic keV ion injections observed by Interball-Auroral during the expansion phase of a substorm, *J. Geophys. Res.*, *104*, 24,929-24,937, 1999.
7. Fuselier, S. A., H. L. Collin, A. G. Ghielmetti, E. S. Claflin, T. E. Moore, M. R. Collier, H. Frey, and S. B. Mende, Localized ion outflow in response to a solar wind pressure pulse, *J. Geophys. Res.*, *107*, doi:10.1029/2001JA000297, 2002.
8. Khan, H., M. R. Collier, and T. E. Moore, Case study of solar wind pressure variations and neutral atom emissions observed by IMAGE/LENA, *J. Geophys. Res.*, *108*, 1093, doi:10.1029/2003JA009977, 2003.
9. Kokubun, S., R. L. McPherron, and C. T. Russell, Triggering of substorms by solar wind discontinuities, *J. Geophys. Res.*, *82*, 74-86, 1977.
10. Kokubun, S., T. Yamamoto, M. H. Acuna, K. Hayashi, K. Shiokawa, and H. Kawano, The GEOTAIL magnetic field experiment, *J. Geomagn. Geoelectr.*, *46*, 7-21, 1994.
11. Moore, T. E., et al., Ionospheric mass ejection in response to a CME,*Geophys. Res. Lett.*, *26*, 2339-2342, 1999.
12. Moore, T. E., et al., The low energy neutral atom imager for IMAGE, *Space Sci Rev.*, *91*, 155-195, 2000.
13. Nishida, A., The GEOTAIL mission, *Geophys. Res. Lett.*, *21*, 2871-2874, 1994.
14. Nosé, M., S. Taguchi, K. Hosokawa, S. P. Christon, R. W. McEntire, T. E. Moore, and M. R. Collier, Overwhelming O^+ contribution to the plasma sheet energy density during the October 2003 superstorm: Geotail/EPIC and IMAGE/LENA observations, *J. Geophys. Res.*, *110*, A09S24, doi:10.1029/2004JA010930, 2005.
15. Williams, D. J., R. W. McEntire, C. Schlemm II, A. T. Y. Lui, G. Gloeckler, S. P. Christon, and F. Gliem, Geotail energetic particles and ion composition instrument, *J. Geomagn. Geoelectr.*, *46*, 39-57, 1994.
16. Winglee, Multi-fluid simulations of the magnetosphere: The identification of the geopause and its variation with IMF, *Geophys. Res. Lett.*, *25*, 4441-4444, 1998.
17. Yau, A. W., W. K. Peterson, and E. G. Shelley, Quantitative parameterization of energetic ionospheric ion outflow, in *Modeling Magnetospheric Plasma*, *Geophys. Monogr. Ser.*, vol. 44, edited by T. E. Moore, and J. H. Waite, Jr., pp. 211-217, AGU, Washington, D. C., 1988.